


Effective-Component Compatibility of Bufei Yishen Formula III Protects Lung Air-Blood Barrier by Regulating the Oxidative Stress: via the Nuclear Factor-E₂-Related Factor 2 Pathway

Kexin Xu^{1,2}, Xuejie Shao^{1,2}, Ruilong Lu^{1,2}, Yixi Liao^{1,2}, Yakun Zhao^{1,2}, Bo Wang^{1,2}, Zhiguang Qiu^{1,2}, Yange Tian^{1,2} 

¹Collaborative Innovation Center for Chinese Medicine and Respiratory Diseases Co-Constructed by Henan Province and Education Ministry of P.R. China, Henan University of Chinese Medicine, Zhengzhou, People's Republic of China; ²Henan Key Laboratory of Chinese Medicine for Respiratory Disease, Henan University of Chinese Medicine, Zhengzhou, People's Republic of China

Correspondence: Yange Tian, Collaborative Innovation Center for Chinese Medicine and Respiratory Diseases Co-Constructed by Henan Province and Education Ministry of P.R. China, Henan University of Chinese Medicine, 156 East Jinshui Road, Jinshui District, Zhengzhou, Henan, People's Republic of China, Email yange0910@126.com

Purpose: Bufei Yishen formula (BYF) is an effective treatment strategy for chronic obstructive pulmonary disease (COPD). Effective-component compatibility of BYF III (ECC-BYF III), composed of 5 active ingredients (ginsenoside Rh1, paeonol, astragaloside, icariin and nobiletin) from BYF, has similar effects to BYF in intervening COPD. The abnormal structure and hypofunction of lung air-blood barrier induces inefficiency gas exchange and promotes development of COPD. However, the role of ECC-BYF III in the air-blood barrier remains unknown. This study dedicated to exploring the effect and mechanism of ECC-BYF III improve structure and function of lung air-blood barrier in COPD.

Methods: A COPD rat model was established to study the treatment of ECC-BYF III against COPD. The protective effect of ECC-BYF III on COPD was evaluated through pulmonary function and lung tissue pathology. The structure damage of the lung air-blood barrier was assessed using electron microscopy and immunofluorescence. Finally, we proved the regulating effect of ECC-BYF III in oxidative via the Nrf2 pathway.

Results: The ECC-BYF III could significantly alleviate reduced pulmonary function, decrease damage of lung tissue and regulate oxidative stress in COPD rats. And ECC-BYF III reduced thickness of respiratory membrane, ameliorated damage of pulmonary capillary endothelial cells (PCECs) and alveolar epithelial cells (AECs) in COPD rats. Also, ECC-BYF III protected the function and normal cell morphology of type I alveolar epithelial cell (AT I) and type II alveolar epithelial cell (AT II) in COPD rats. Lastly, ECC-BYF III was indicated to adjust the Nrf2 pathway to improve oxidative stress and protect lung air-blood barrier in COPD rats.

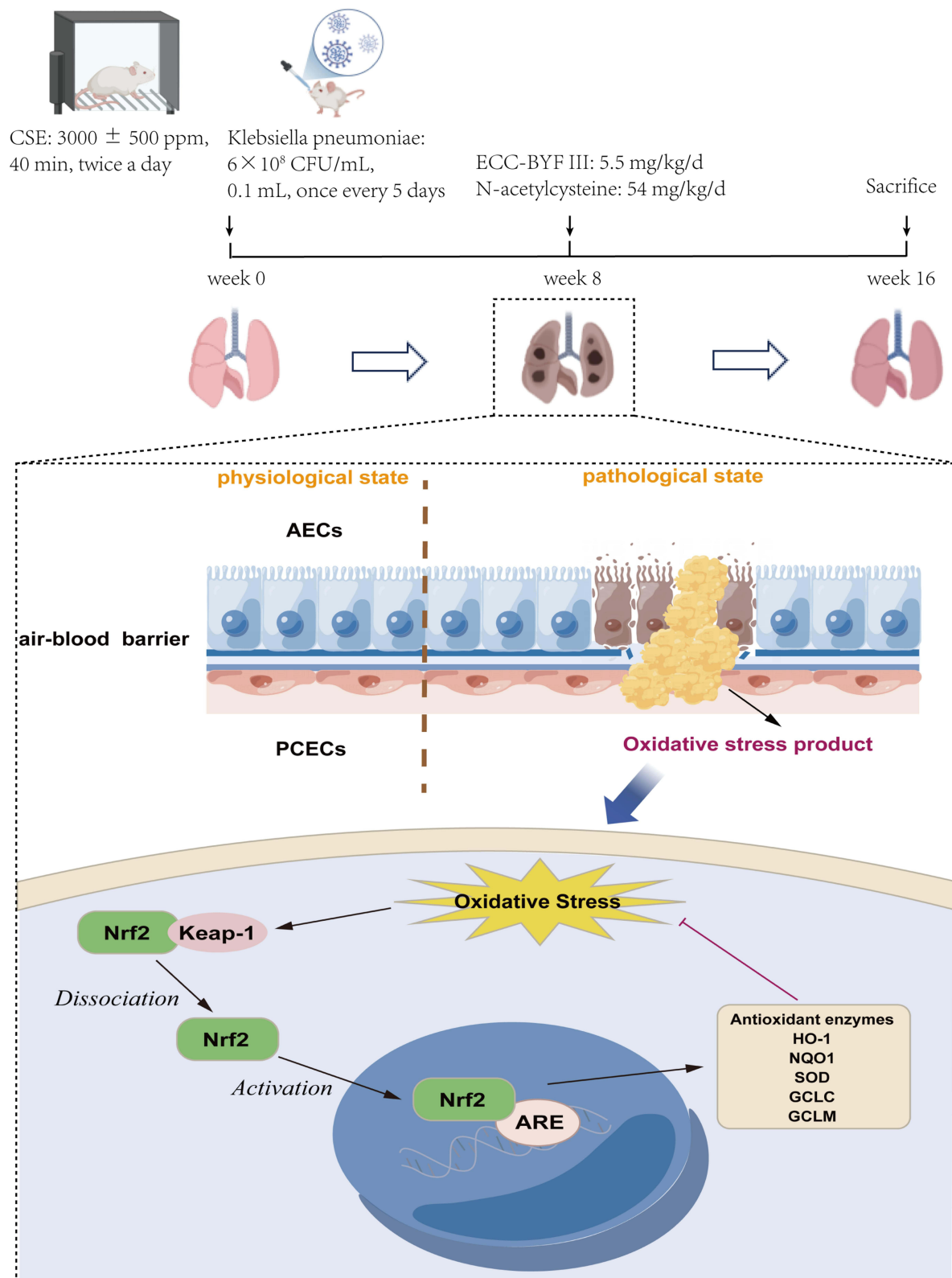
Conclusion: ECC-BYF III protects lung air-blood barrier in COPD by regulating oxidative stress via Nrf2 pathway.

Keywords: effective-component compatibility of bufei yishen formula III, chronic obstructive pulmonary disease, lung air-blood barrier, oxidative stress, Nrf2 pathway

Introduction

Chronic obstructive pulmonary disease (COPD), a common preventable and treatable respiratory disease, is characterized as persistent respiratory symptoms and airflow limitation.¹ Nowadays, the treatment strategies of COPD, including bronchodilators and glucocorticoid, still cannot protect normal gas exchange function of lung air-blood barrier and delay the development of COPD.¹ The lung air-blood barrier is the main place for gas exchange between the human body and the external environment, which is mainly composed of alveolar epithelial cells (AECs) and pulmonary capillary endothelial cells (PCECs). Abnormal gas exchange caused by damage of the lung air-blood barrier is the main

Graphical Abstract



pathological changes in the development of COPD.² In the early stage of damage, self-repair of AECs and PCECs can inhibit and improve injury to a certain extent. However, long-term stimulation, such as air pollution, cigarette pellet and microorganism, can cause AECs and PCECs to release a large amount of cytokines breaking the adhesion and connections of AECs and PCECs and damage of lung air-blood barrier, leading to a series of acute and chronic respiratory diseases represented by COPD.^{2,3}

Oxidative stress causes damage to AECs and PCECs function, abnormal lung air-blood barrier function, and promotes the occurrence and development of COPD.^{4,5} Apoptosis of AECs and PCECs caused by cigarette smoke and harmful gases produces a large amount of reactive oxygen species (ROS).⁶ Under normal circumstances, ROS is degraded by antioxidant enzymes in the body. When a large amount of reactive oxygen species is produced that exceeds the body's removal ability, ROS will accumulate in the body, causing imbalance of oxidation-antioxidation.⁷ The role of Nrf2 signaling in oxidative stress in COPD has been reported.⁸ Zhu Wentao et al confirmed that CSE stimulation could reduce the expression of Nrf2 and NQO1 in 16HBE cells, leading to severe oxidative stress and ultimately cell apoptosis.⁹ The increase in the abundance of fine particulate matter (PM_{2.5}) in the environment could produce excess ROS and trigger NOX4/Nrf2 redox imbalance, reducing mitochondrial membrane potential (MMP) and aggravating mitochondrial fragmentation.¹⁰ Disruption of oxidative balance in the body increased susceptibility to acute exacerbations of COPD. However, the role of Nrf2 in the air-blood barrier in COPD is still less reported.

Traditional Chinese medicine (TCM) is an effective treatment strategy for COPD patients. Bufe Yishen formula (BYF), a combination of Chinese herbs, has obvious therapeutic effects for COPD including improving lung function and inhibiting the inflammatory response.¹¹ Previous studies had shown that BYF could improve pulmonary function in COPD rats and can also reduce the thickening of the air-blood barrier in COPD rats.^{12,13} Effective-component compatibility of Bufe Yishen formula III (ECC-BYF III) is composed of ginsenoside Rh1, nobiletin, paeonol, astragaloside and icariin, which are active ingredients screened from BYF. Previous researches have confirmed that ECC-BYF III can improve the lung function and alleviate the oxidative stress state of COPD rats.¹⁴

In the study, we established a COPD rat model through cigarette smoke exposure (CSE) combined with repeated *Klebsiella pneumoniae* infection.¹⁵ Then, the effects of ECC-BYF III on lung function and lung air-blood barrier were evaluated in COPD rats. Furthermore, we verified the regulation of ECC-BYF III on oxidative stress via the Nrf2 pathway in COPD rats, which was underlying mechanism to protect the lung air-blood barrier.

Materials and Methods

Chemicals and Reagents

Cigarettes were purchased from Henan Tobacco Industry (Hongqi Canal[®] Filter tip cigarette; tar: 10 mg; nicotine content: 1.0 mg; carbon monoxide: 12 mg; Zhengzhou, China). *Klebsiella pneumoniae* (46117–5a1) was provided by National Center for Medical Culture Collections (Beijing China). Ginsenoside Rh1 (CHB180608), paeonol (MUST-16071405), astragaloside (MUST-17022804) and icariin (MUST-16111710) were purchased from Chengdu Must Bio-Technology (Chengdu, China). Nobiletin (HL-20170312) was purchased from Xi an Huiling Bio-Technology (Xi an, China). The antibody for rat of ZO-1 (AF5145), Claudin-5 (AF5216) and SP-D (DF13601) were purchased from Affinity Bioscience (America). The antibody for rat of Ang-2 (Sc-74402) was purchased from Santa Cruz Biotechnology (America). The antibody for rat of Nrf2 (GTX1033322), NAD(P)H: quinone oxidoreductase 1 (NQO1) (GTX100235), SOD2 (GTX116093), GCLC (GTX66057) and GCLM (GTX114075) were purchased from Gene Tex (America). The antibody for rat of Heme Oxygenase-1 (HO-1) (43966) was purchased from CST (America). The malondialdehyde (MDA) assay kit (TBA method) (A003-1-2) and total superoxide dismutase (T-SOD) assay kit (Hydroxylamine method) (A001-1-2) were purchased from Nanjing Jiancheng Bioengineering Institute (Nanjing, China). N-acetylcysteine was purchased from Zambon S.p.A (Italia).

COPD Rat Model Establishing

Sprague-Dawley rats were provided by Beijing Vital River Laboratory Animal Technology Co., Ltd (220 ± 20 g, No.110011211105823815, Beijing, China). A total of 48 SD rats were housed under standardized environment conditions and given food and water ad libitum for 7 days, then were randomly assigned to four experimental groups: normal group,

model group, ECC-BYF III group, and N-acetylcysteine (NAC) group ($n = 12$ for each). The COPD rat model was established by cigarette smoke inhalation and repetitive bacterial infection.¹⁵ The rats were exposed to CSE (3000 ± 500 ppm) for 40 minutes twice a day for 8 weeks. *Klebsiella pneumoniae* was resuspended in physiological saline, and the concentration was set to 6×10^8 CFU/mL. *Klebsiella pneumoniae* suspension was instilled through the nasal cavity, alternating between the left and right nasal cavities. Each rat received 0.1 mL of *Klebsiella pneumoniae* suspension once every 5 days.

The study was conducted according to *Laboratory animal-Guideline for ethical review of animal welfare GBT/35892-2018*. The research procedure was approved by the Experimental Animal Care and Ethics Committees of the First Affiliated Hospital of Henan University of Chinese Medicine with the ethical review approval number YFYDW2019031.

Drug and Treatment

From week 9, the ECC-BYF III group rats were treated with ECC-BYF III (made from ginsenoside Rh1, astragaloside, icariin, paeonol and nobiletin) at 5.5 mg/kg/d. The NAC group were treated with N-acetylcysteine at 54 mg/kg/d.^{16,17} The normal group and model group rats were intragastrically administered 10 mL/kg/d 0.5% sodium carboxymethyl cellulose. The equivalent dosage of N-acetylcysteine (54 mg/kg/d) was calculated according to the following formula (D: dose; K: body shape index, $K = A/W^{2/3}$, A: surface area in m^2 , W: weight in kg):

$$D_{\text{rat}} = D_{\text{human}} \times (K_{\text{rat}}/K_{\text{human}}) \times (W_{\text{rat}}/W_{\text{human}})^{2/3}$$

At week 17, 4 groups rats were sacrificed after intraperitoneal injection of 2% pentobarbital sodium at 40 mg/kg.

Weight and Pulmonary Function Tests

During the preparation and administration of the rat model at 0–16 weeks, the rat weight was measured every week. The animal pulmonary function detection system (DSI, USA) was used to detect rat tidal volume (TV), peak expiratory flow (PEF) and 50% tidal volume expiratory flow (EF50), once every 4 weeks.

Lung and Airway Tissues Histopathology

The lung tissues were fixed in 4% paraformaldehyde solution. Next, the tissues were cut and embedded in paraffin and made slices. Then, the lung tissues slices were stained with hematoxylin and eosin, and were observed by light microscope (Olympus, Tokyo, Japan). The mean linear intercept (MLI) and mean alveolar numbers (MAN) were considered as lung tissue injury. Under microscopy ($\times 200$), six visual field were taken in each slice, and the alveolar number and the linear intercept in a fixed area of visual field were measured. $MAN (/mm^2) = Na/A$. Na is the number of pulmonary alveoli in each visual field. A is the area of the visual field. Then, we made a cross (+) under the visual field and counted the number of alveolar septums on the cross. $MLI (\mu m) = L/Ns$. Ns is the number of alveolar septums. L is total length of the cross. Airway wall thickness (AWT) was considered as airway remodeling. Under microscopy ($\times 200$), three visual field which include airway (100–300 μm in diameter) were taken in each slice, and select three internal diameters and corresponding external diameters of the airways, respectively, subtract and average value, then divide by 2, and this means the airway wall thickness.

Measurements of T-SOD and MDA in Lung Tissue and Serum

The level of T-SOD and MDA in lung tissue and serum were detected using MDA assay kit and T-SOD assay kit and quantified according to the manufacturer's protocol.

Ultrastructure of Lung Tissue The lung tissue was cut into 1 mm \times 1 mm \times 1 mm small pieces, and fixed with 2.5% glutaraldehyde, then fixed with 1% osmic acid. The tissue was cut and embedded in Epon218 and made slices. The ultrastructure of air-blood barrier, capillary endothelial, Type I alveolar epithelial cell (AT I) and Type II alveolar epithelial cell (AT II) were observed by JEM-1400 transmission electron microscope.

Immunofluorescence Staining

The tissue slices were blocked with 3% BSA for 30 min. Then, anti-rabbit antibodies against AQP-5, SP-D and CD31 (1:1000, proteintech) were added at 4°C overnight. Moreover, the tissue slices were treated with fluorescein-conjugated secondary antibody (1:1000, proteintech) in a dark place for 1 h. Finally, the laser confocal microscope was used for detection (LSM700, Carl Zeiss, Germany).

Immunohistochemistry

ZO-1 (1:500) and claudin-5 (1:500) were assessed through immunohistochemical staining. And the secondary antibody was biotin-labeled goat anti-rabbit IgG (1:100). The experimental procedures were conducted in accordance with the instructions provided in the immunohistochemistry kit manual (SA2002, BOSTER). The captured images were digitalized by calculating the integrated optical density (IOD) with Image-Pro Plus 6.0 software.

Western Blot

The protein levels of GAPDH (1:5000), laminB (1:1000), ZO-1 (1:1000), SP-D (1:1000), claudin-5 (1:1000), Nrf2 (1:1000), Ang-2 (1:1000), HO-1 (1:1000), NQO1 (1:1000), SOD2 (1:1000), GCLC (1:1000) and GCLM (1:1000) in lung tissue were measured by Western blot.

Statistical Analysis

The experimental data were analyzed by SPSS v21.0. Comparison among groups was performed by One-way ANOVA of variance with an appropriate post hoc test. If the variances were homogeneous, LSD method was performed. If the variances were inconsistent, dunnett'T3 test was performed. The mean \pm SEN were used as the data present presentation. A p-value of <0.05 was set for statistically significant difference.

Results

ECC-BYF III Could Effectively Improve Lung Function and Pathological Injury in COPD Rats

Pulmonary function testing is the basis for the diagnosis of COPD, and histopathological changes and oxidative stress are important features of COPD. Therefore, we studied the effect of ECC-BYF III on COPD rats by comparing the lung function, pathological changes and oxidative stress of ECC-BYF III-treated rats and untreated rats.

During the 16-week experiment, the rats in the normal group exhibited smooth and glossy fur, a good mental state, normal movement, a normal diet, and consistent weight gain. After 2 weeks of modeling, the rats in the model group displayed yellowish fur, reduced gloss, and a decline in spirits. By the 4th week of modeling, the activity level of the model rats significantly decreased, and they showed signs of mental fatigue. At the end of the 8-week modeling period, the weight of the rats in the model group had significantly decreased compared to the rats in the normal group. In contrast, the rats in the ECC-BYF III group and the NAC group demonstrated significant improvement in mental state, increased activity, and a substantial increase in body weight after 16 weeks of intervention, surpassing the improvements observed in the model group (Figure 1a).

TV, PEF, and EF50 are important indicators for assessing dyspnea severity.¹⁸ Over a period of 0 to 4 weeks, lung function in each group of rats improved as their body weight increased. However, by the 8th week, the TV, PEF, and EF50 of rats in the model group showed a decrease compared to the normal group. By week 12, the TV, PEF, and EF50 of rats in the model group had decreased significantly compared to the normal group. At the 16th week, the TV, PEF, and EF50 of rats in the model group were significantly lower than those in the normal group. However, the TV, PEF, and EF50 of rats in the ECC-BYF III group and NAC group showed a significant increase compared to the model group (Figure 1b–d).

To assess alveolar damage, MAN and MLI were used, while airway wall thickness was used to evaluate airway remodeling. The lung tissues of rats in the model group exhibited severe pathological changes, including decreased

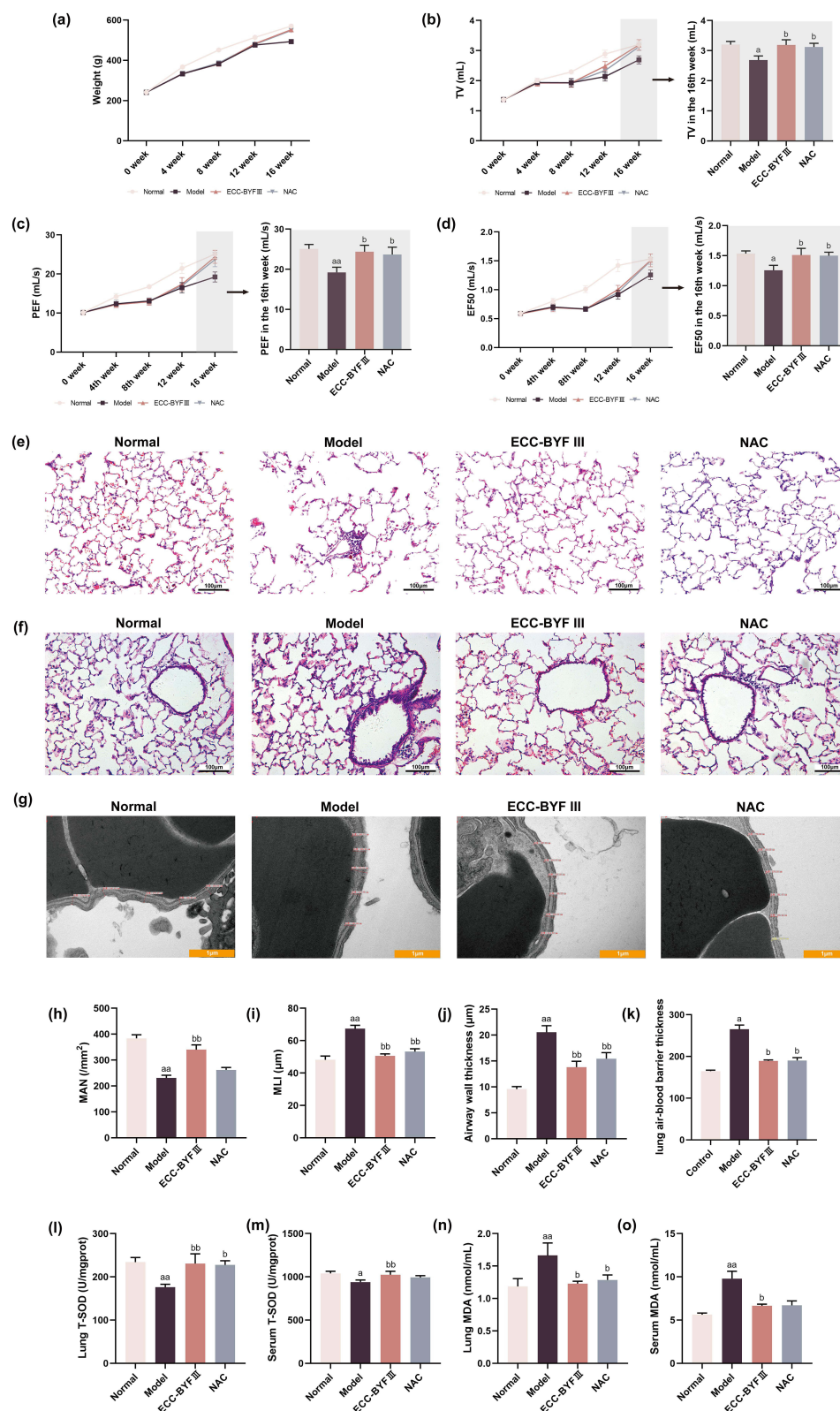


Figure 1 ECC-BYF III can effectively improve disease severity lung in COPD rats. **(a)** Changes of weight in all groups, **(b)** Changes of tidal volume (TV) in all groups, **(c)** Changes of peak expiratory flow (PEF) in all groups, **(d)** Changes of expiratory flow at 50% tidal volume (EF50) in all groups, **(e)** Photographs of pulmonary alveolus histopathology (HE, $\times 200$), **(f)** Photographs of pulmonary airway histopathology (HE, $\times 200$), **(g)** Electron microscope images of lung air-blood barrier morphology and thickness in all groups ($\times 30,000$), **(h–j)** Changes of MAN, MLI and airway wall thickness, **(k)** Changes of lung air-blood barrier thickness in all groups, **(l)** Changes of T-SOD in lung tissue, **(m)** Changes of T-SOD in serum, **(n)** Changes of MDA in lung tissue, **(o)** Changes of MDA in serum. The values are expressed as mean \pm SE, ($n = 8$). ^a $P < 0.05$ vs the control group, ^{aa} $P < 0.01$ vs the control group, ^{bp} $P < 0.05$ vs the model group, ^{bbp} $P < 0.01$ vs the model group.

MAN, increased MLI, and increased airway wall thickness, compared to the normal group. However, these changes were significantly improved in the ECC-BYF III and NAC groups (Figure 1e–j).

Observing the morphology of lung air-blood barrier under an electron microscope. In the normal group, the lung air-blood barrier had a clear structure, distinct layers, and was relatively uniform. The liquid layer containing lung surfactant was full, and the basement membrane layer, interstitial layer, epithelium, and endothelial layer were clearly visible. The structural layer of the model group was uneven, with blurred edges, occasional breaks, uneven liquid layer, and significant thickening of the epithelial basement membrane layer, the interstitial layer between the alveoli and capillaries, and the capillary basement membrane layer. Compared with the model group, the ECC-BYF III group and the NAC group had a clearer structural layer, the thickness of the air-blood barrier was reduced, and the ultrastructural damage was improved. Through statistical analysis, it was found that the lung air-blood barrier was significantly thickened in the model group, and the thickness of the lung air-blood barrier was reduced in the ECC-BYF III group and NAC group (Figure 1g–k).

Compared with the normal group, the T-SOD activity in the lung tissue and serum of rats in the model group was significantly reduced, and the MDA expression was significantly increased. Compared with the model group, the T-SOD activity in the lung tissue and serum of rats in the ECC-BYF III group was significantly increased, and the MDA expression was significantly decreased; the T-SOD activity in the lung tissue of the NAC group was significantly increased, and the MDA expression was decreased (Figure 1l–o).

ECC-BYF III Could Improve the Ultrastructural Damage of Air-Blood Barrier in COPD Rats

PCECs in the Normal group had flat cells, regular nuclei, visible ribosomes in the cytoplasm, many rough endoplasmic reticulum vesicles, and uniform thickness of cell membrane. In the model group, the vascular endothelial gap became wider, the cells were arranged in disorder, the cell shape was irregular, the membrane structure was fuzzy, the edges were unclear, and cell debris was occasionally seen. Compared with the model group, the structure of PCECs in the ECC-BYF III group and NAC group was improved and the morphology was restored (Figure 2a).

AT I in normal group had a complete structure and smooth surface. The nucleus-containing part of the cells was thicker and protrudes into the alveolar cavity. The cytoplasm of the non-nucleated part was thin. Ribosomes and more clear phagocytosis vesicles can be seen in the cytoplasm. AT II in normal group had a clear structure, neatly arranged villi, a large number of lamellar bodies, a large number of mitochondria, and clear and neatly arranged mitochondrial ridges. AT I had a fuzzy structure, unclear edges, rough surface, and decreased number of swallowed vesicles in model group. The structure of AT II was unclear, the lamellar bodies fall off and become vacuoles, the number was reduced, the mitochondria appear pyknotic or swollen, the ridges were blurred, and the arrangement was uneven. Compared with the model group, the structures of AT I and AT II in the ECC-BYF III group and NAC group were improved, the vacuolization of lamellar bodies in AT II was improved, the number of mitochondria increased, and the morphology was restored (Figure 2b and c).

ECC-BYF III Could Improve the Ultrastructural Damage of Air-Blood Barrier in COPD Rats

Immunofluorescence was used to double-stain the AT I marker AQP-5 and the PCECs marker CD31, and the AT II marker SP-D and the vascular endothelial cell marker CD31. IF AQP5/CD31 results showed that compared with the normal group, the fluorescence intensity of type I alveolar epithelial cell marker AQP-5 was significantly reduced and the fluorescence intensity of the vascular endothelial cell marker CD31 had an upward trend in the model group. Compared with the model group, the fluorescence intensity of AQP-5 increased and the fluorescence intensity of CD31 decreased in the ECC-BYF III group and NAC group (Figure 3). IF SP-D/CD31 results showed that compared with the normal group, the fluorescence intensity of type II alveolar epithelial cell marker SP-D was significantly reduced and the fluorescence intensity of the vascular endothelial cell marker CD31 was significantly increased in the model group. Compared with the model group, the fluorescence intensity of SP-D increased in the BYF III group and the NAC group, while the CD31 fluorescence intensity decreased (Figure 4).

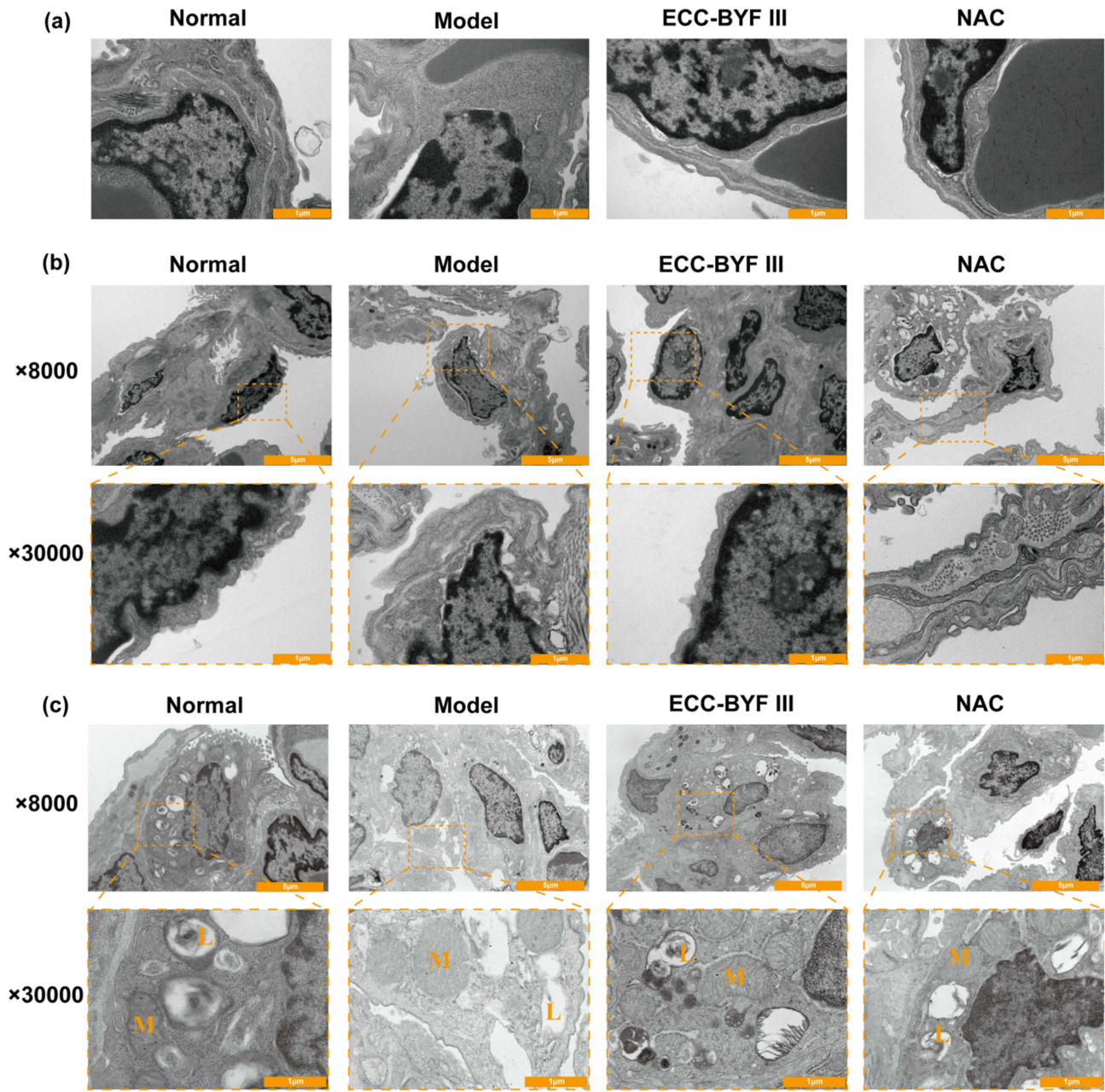


Figure 2 ECC-BYF III can improve the ultrastructural damage of air-blood barrier in COPD rats. (a) Electron microscope images of pulmonary capillary endothelial cells (PCECs) morphology in all groups, (b) Changes of type I alveolar epithelial cell (AT I) structure in all groups, (c) Changes of type II alveolar epithelial cell (AT II) structure in all groups. In (b and c), the pictures on the left of each group are $\times 8000$, and the dotted yellow box on the right is $\times 30000$. M: mitochondrion, L: lamellar body. The values are expressed as mean \pm SE, (n = 8).

Tight junction-related indicators ZO-1 and claudin-5 were detected using immunohistochemistry. ZO-1 and claudin-5 were widely and uniformly present in the lung tissue of rats in the normal group, compared with the normal group, the lung tissue of rats in the model group ZO-1 and claudin-5 were significantly reduced, with only a small amount of expression. Compared with the model group, the expression of ZO-1 and claudin-5 in the lung tissue of rats in the ECC-BYF III group and NAC group was significantly increased, and their IOD values were significantly increased (Figure 5a).

WB was used to detect lung air-blood barrier and tight junction-related proteins. Compared with the normal group, the protein expressions of ZO-1, SP-D, and claudin-5 in the lung tissue of rats in the model group were significantly

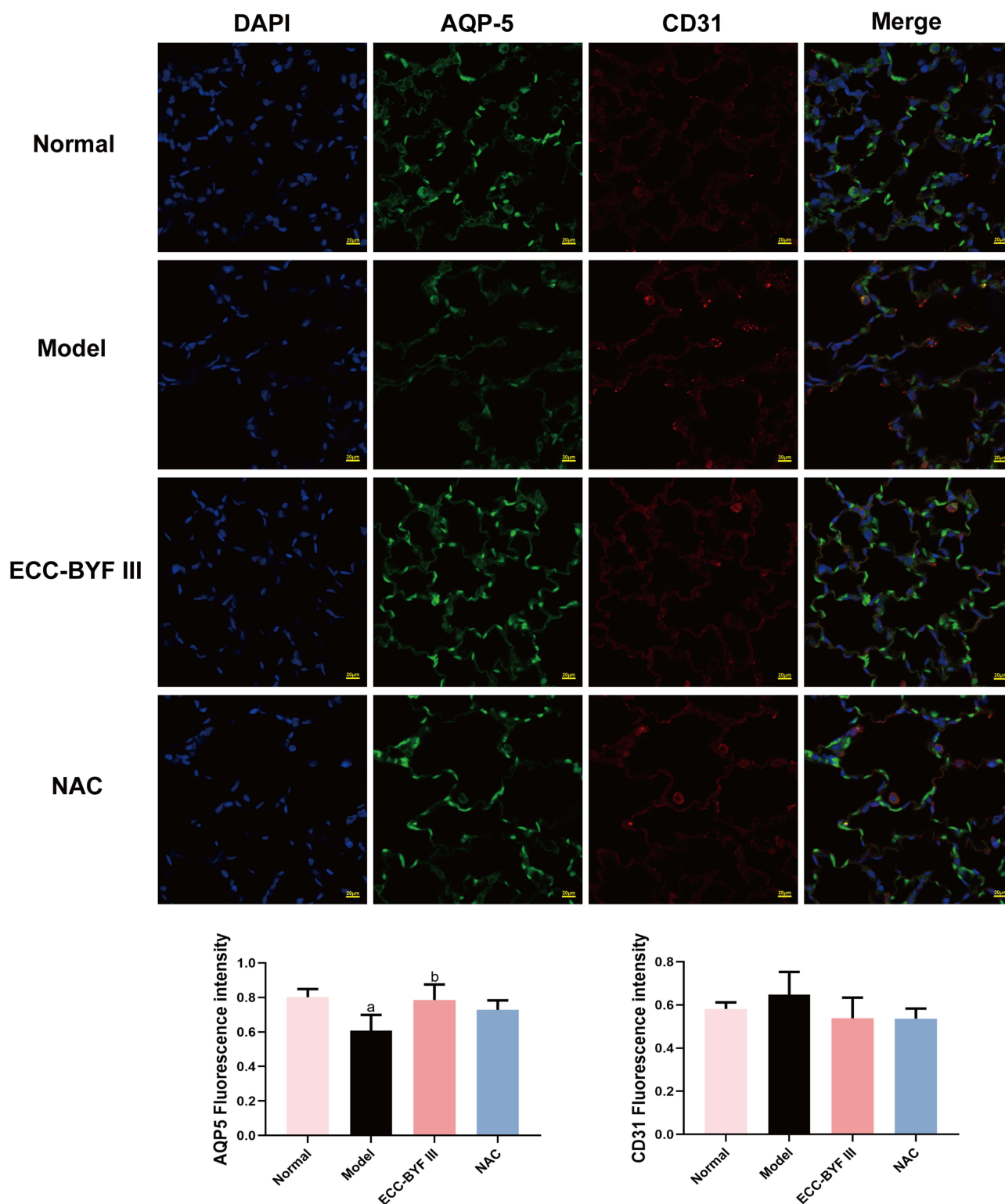


Figure 3 Changes of AQP5/CD31 expression in lung tissues of rats in all groups. ($\times 400$). ^a $P < 0.05$ vs the control group, ^b $P < 0.05$ vs the model group.

decreased, and the expression of Ang-2 was significantly increased. Compared with the model group, the expressions of ZO-1, SP-D, and claudin-5 were significantly increased, and the expression of Ang-2 was significantly decreased in the lung tissue of rats in ECC-BYF III group and NAC group (Figure 5b).

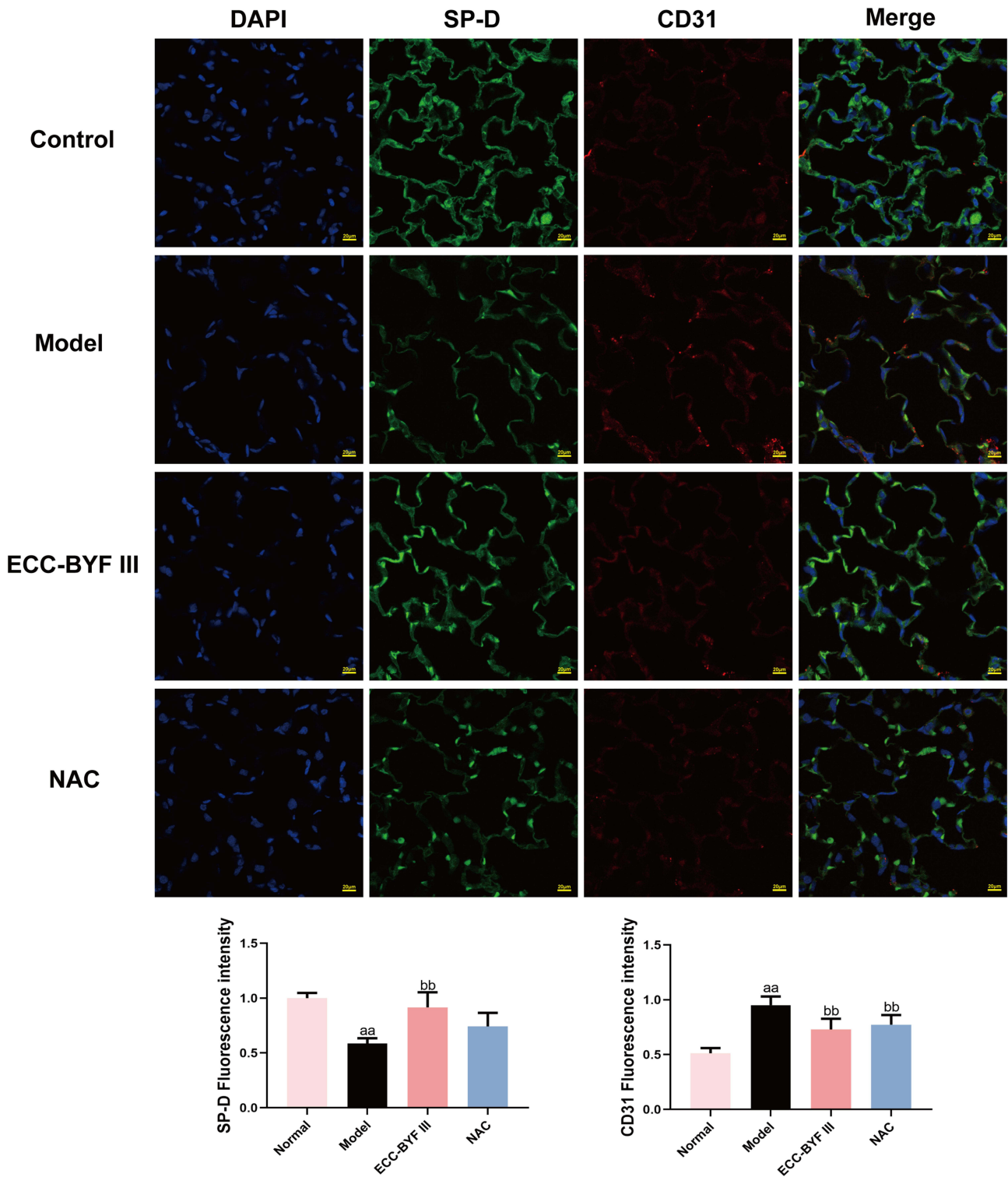


Figure 4 Changes of SP-D/CD31 expression in lung tissues of rats in all groups. (×400). ^{aa}*p* < 0.05 vs the control group, ^{bb}*p* < 0.05 vs the model group.

ECC-BYF III May Improve Lung Air-Blood Barrier Damage in COPD Rats by Activating Nrf2 Pathway

WB was used to detect proteins related to the lung air-blood barrier and tight junctions. Compared with the normal group, the expression of Nrf2 protein in the nucleus of the lung tissue of rats in the model group showed a downward trend, and

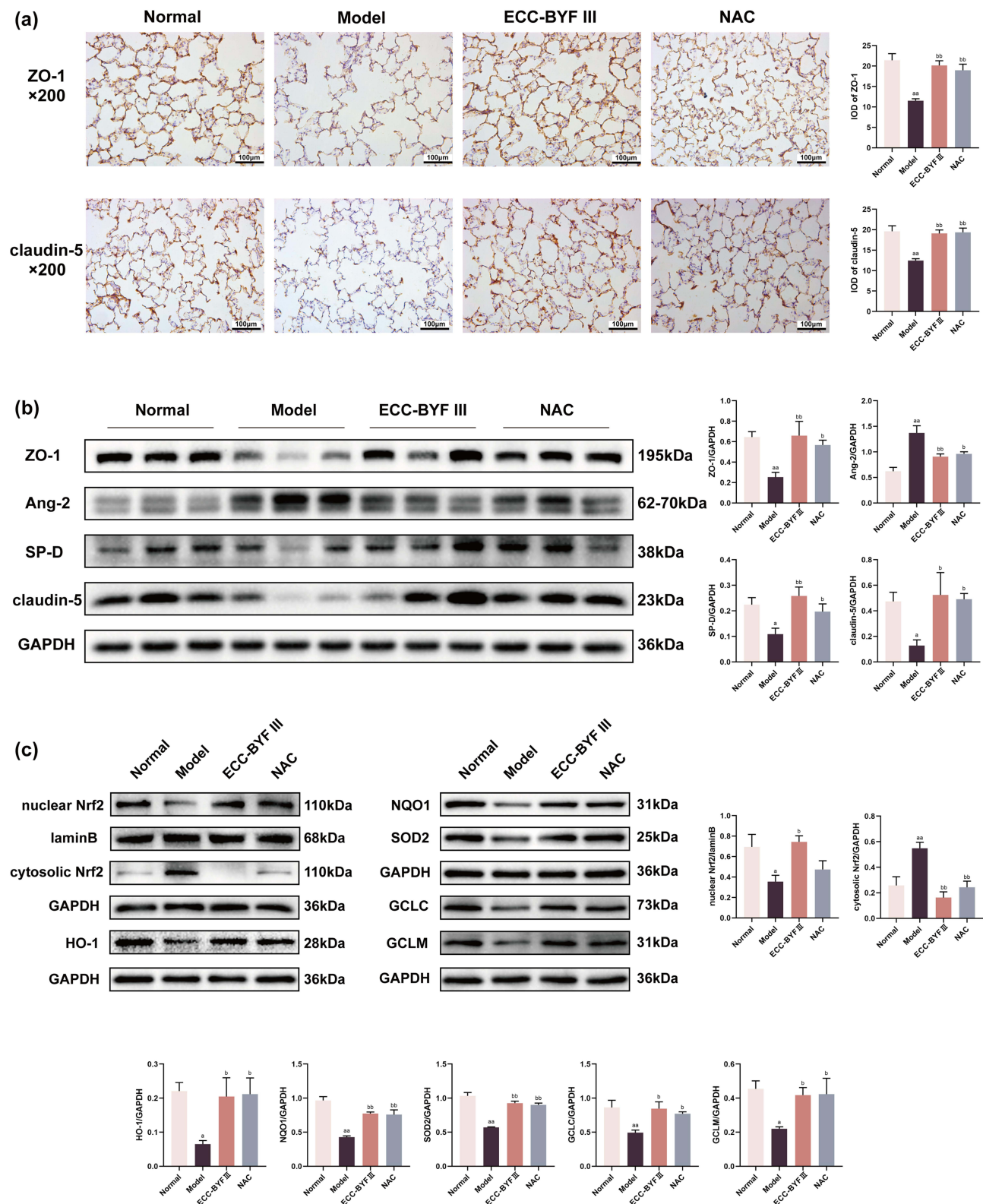


Figure 5 ECC-BYF III improved the structural and functional damage of air-blood barrier through Nrf2 pathway. **(a)** The expression level of ZO-1 and claudin-5 in lung tissue tested using immunohistochemistry ($\times 200$) and IOD of ZO-1 and claudin-5 in lung tissue of rats in all groups ($n = 8$), **(b)** ZO-1, Ang-2, SP-D and claudin-5 protein expression bands and relative protein expressions in lung tissue of rats in all groups ($n = 3$), **(c)** nuclear Nrf2, cytosolic Nrf2, HO-1, NQO1, SOD2, GCLC and GCLM protein expression bands and relative protein expressions in lung tissue of rats in all groups ($n = 3$). The values are expressed as mean \pm SE. ^a $P < 0.05$ vs the control group, ^{aa} $P < 0.01$ vs the control group, ^b $P < 0.05$ vs the model group, ^{bb} $P < 0.01$ vs the model group.

the expression of Nrf2 protein in the cytoplasm showed an upward trend. Compared with the model group, the expression of Nrf2 protein in the nucleus increased significantly in the ECC-BYF III group, while the expression of Nrf2 protein in the cytoplasm of the ECC-BYF III group and NAC group decreased significantly. Compared with the normal group, the protein expressions of HO-1, NQO1, SOD2, GCLC, and GCLM in the lung tissue of rats in the model group were significantly decreased. Compared with the model group, the expressions of HO-1, NQO1, SOD2, GCLC, and GCLM all increased significantly in ECC-BYF III group and NAC group (Figure 5c).

Discussion

The lung air-blood barrier is a site formed by the tight connections between alveoli and capillaries. It is mainly composed of alveoli and capillaries. It is an important place for gas exchange in the lungs, also the main structure that forms the alveolar septum and plays an important role in maintaining normal respiratory function.¹⁹ The lung air-blood barrier is composed of six layers, including the liquid layer containing pulmonary surfactant, the alveolar epithelial layer, the epithelial basement membrane layer, the interstitial layer between the alveoli and capillaries, the capillary basement membrane layer, and the capillary endothelium.⁷ AECs and PCECs are the main component cells of the lung air-blood barrier structure. They work together to maintain the normal function of the lung air-blood barrier and the normal structure of the alveoli.¹⁹ The key link in the destruction of the lung air-blood barrier that promotes the development of COPD is mainly related to inflammatory response and oxidative stress. Inhalation of cigarettes and harmful substances causes inflammation and oxidative stress, directly damaging AECs.²⁰ Damaged AECs secrete a large of cytokines, such as IL-6, which can promote pulmonary inflammatory response and reduce lung function. At the same time, IL-6 participates in the migration of neutrophils into lung tissue, which further aggravate the impact of inflammatory response and worsen the progression of COPD.^{21,22} Moreover, cigarette smoke stimulation reduces the secretion of pulmonary surfactant and changes the composition of pulmonary surfactant.²³ The lipids of pulmonary surfactant are significantly changed in COPD patients. The abnormal lipid composition destroys the function of pulmonary surfactant, and the abnormal function of phospholipids increased alveolar surface tension, leading to alveolar tissue destruction, thereby aggravating the damage to the lung air-blood barrier.²⁴ In patients with early COPD, vascular endothelial dysfunction exists. Vascular endothelial dysfunction and the imbalance between vasodilation and vasoconstriction are key factors in the destruction of the pulmonary vasculature in patients with COPD. Cigarette smoke is the cause of destruction of the pulmonary vasculature. Inflammation and hypoxia can further lead to vascular damage. Various factors work together to promote the exacerbation of COPD.²⁵

In this study, we observed the cellular morphology of the lung air-blood barrier through transmission electron microscopy. After exposure to cigarette smoke and bacterial infection, the lung air-blood barrier of COPD model rat was significantly thickened, and the structure of the air-blood barrier was uneven. PCECs were arranged disorderly, and the cell morphology was irregular, which caused the vascular endothelial gap wider. AT I structure also was fuzzy, and AT II structure was unclear. After treatment of ECC-BYF III, the structure of the air-blood barrier in rats became clearer, and the structure of AT I, AT II and PCECs improved. Moreover, the vacuolization of lamellar bodies in AT II improved, and the number of mitochondria increased. These evidences suggested that ECC-BYF III could promote the renewal of damaged cells. Then, we evaluated the structural integrity of the lung air-blood barrier. ZO1 was an important component of tight junctions, regulating and maintaining cell barrier function together with other cell junction proteins, and was considered as one of the important indexes for evaluating tight junctions and tissue permeability.²⁶ Claudin-5 was also a tight-junction protein, which was expressed on both AECs and PCECs, and interacted with ZO-1 to affect the homeostasis of the tight-junction of the lung air-blood barrier.²⁷ We found that ECC-BYF III could reverse the decrease in ZO-1 protein and claudin-5 protein caused by cigarette smoke exposure and bacterial infection, indicating that ECC-BYF III could restore the integrity of the damaged lung air-blood barrier. Further, we evaluated the function of key cells of the lung air-blood barrier. Aquaporin 5 was a cell membrane transport protein related to fluid transport. It was mainly distributed on the top membrane surface of AT I and was an important protein that reflects the function of AT I.^{26,27} As a type of pulmonary surfactant, SP-D was an important functional protein secreted by AT II and attached to the surface of AT I. It could be used as a marker to evaluate the degree of AT II damage and indirectly reflect the structural and functional damage of alveolar epithelium.^{28,29} PECAM-1/CD31 existed in the tight junctions of endothelial cells and was

a marker of vascular endothelial cells.^{30,31} In this study, we confirmed that cigarette smoke and bacterial infection caused different degree changes of Aquaporin 5, SP-D and CD31 protein expression, which is consistent with the conclusions of previous studies. After treatment with ECC-BYF III, the expressions of these proteins were restored, meaning that the function of the cells were improved.

COPD patients are continuously exposed to exogenous or endogenous oxidants, and the activity of enzymatic antioxidants and levels of non-enzymatic antioxidants are reduced. The combined effect of the two directly damages lung tissue, causing oxidation and inactivation of antiproteases, activation of inflammatory cells and increased gene expression of pro-inflammatory mediators, thus promoting the occurrence and development of COPD.^{32,33} Nrf2 is an important transcription factor that regulates antioxidant enzymes, regulates oxidative stress, and maintains intracellular oxidant-antioxidant homeostasis.³⁴ Nrf2 is ubiquitinated under the action of Kelch-like ECH-associated protein 1 (Keap-1) and rapidly degraded by protease. When stimulated by ROS, Nrf2 dissociates from Keap-1 and translocates into the

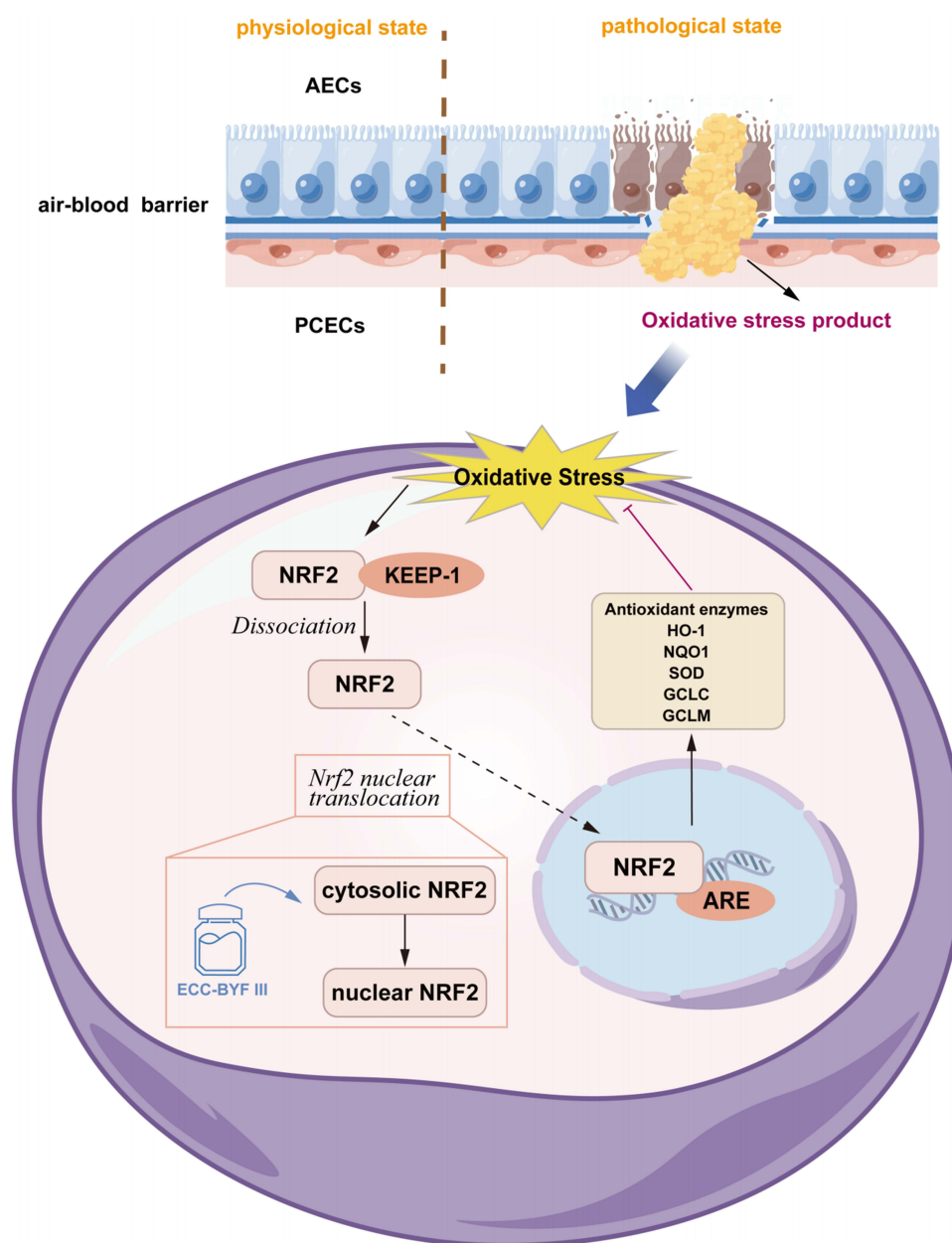


Figure 6 ECC-BYF III alleviates oxidative stress in lung air-blood barrier of COPD.

nucleus, binds to ARE in the nucleus, activates the expression of downstream antioxidant enzymes, and enhances the antioxidant capacity of cells.³⁵ When oxidative products such as ROS exceed the body scavenging capacity, the overload of oxidative products leads to the oxidation/antioxidant imbalance regulated by Nrf2, and nuclear migration of Nrf2 is reduced, the downstream antioxidant enzyme expression is unbalanced, and the body presents a state of oxidative stress.³⁶ HO-1 and NQO1 are important protective proteases downstream of Nrf2.³⁷ When oxidative stress occurs, activated Nrf2 induces the expression of SOD2 and other antioxidant factors. By increasing the expression of NQO1 and glutamine cysteine ligase (GCL) subunits GCLC and GCLM, Nrf2 accelerates the clearance of oxidizing substances, such as ROS and MDA, and promotes the generation of antioxidant enzymes, such as SOD and GSH, maintaining the oxidant-antioxidant homeostasis.^{38–40} Consistent with these conclusions, we found a reduction in nuclear transfer of Nrf2 in COPD rat lung tissue. After treatment with ECC-BYF III, the nuclear transfer of Nrf2 was restored, and the level of SOD2, HO-1, NQO1, GCLC and GCLM were increased. These results suggest that ECC-BYF III could reverse the decline of nuclear transfer of Nrf2 induced by CSE and *Klebsiella pneumoniae*, maintain the balance of oxidation and antioxidant state by increasing levels of antioxidant and clearing oxidation products.

Although the role of ECC-BYF III in protecting lung blood-air barrier damage in COPD has been confirmed, there are still some limitations that need to be addressed with appropriate methods. This study has demonstrated the regulatory effects of ECC-BYF III on oxidative stress and Nrf2 signaling, but whether ECC-BYF III indeed ameliorates lung air-blood barrier damage by modulating Nrf2 signaling still requires further molecular biology experiments for validation. Co-culture of alveolar epithelial cells and vascular endothelial cells in vitro may contribute to a deeper exploration of the mechanism of ECC-BYF III. Meanwhile, the rational application of Nrf2 inhibitors within the co-culture system can help us clarify the role of the Nrf2 signaling pathway in the protection of the lung blood-air barrier injury by ECC-BYF III.

Conclusion

In this study, we confirmed the protective effect of ECC-BYF III on the lung air-blood barrier in COPD rats. ECC-BYF III could improve the oxidative stress imbalance in the lung tissue of COPD rats, and Nrf2 signaling may be the potential mechanism (Figure 6). This study provided a new perspective for the treatment of COPD and new ideas for the research on component compatibility of TCM.

Data Sharing Statement

The datasets used and/or analysed during the current study are available from the corresponding author on reasonable request.

Ethics Approval

The study was conducted according to *Laboratory animal-Guideline for ethical review of animal welfare GBT/35892-2018*. The research procedure was approved by the Experimental Animal Care and Ethics Committees of the First Affiliated Hospital of Henan University of Chinese Medicine with the ethical review approval number YFYDW2019031.

Acknowledgments

This study was supported by Henan Key Laboratory of Chinese Medicine for Respiratory Disease, Co-construction Collaborative Innovation Center for Chinese Medicine and Respiratory Diseases by Henan & Education Ministry of P.R., the authors are grateful to lab members for their insightful comments on the work. Also, the authors are grateful to the Electron Microscope Center of Henan University of Chinese Medicine for the support.

Author Contributions

All authors made a significant contribution to the work reported, whether that is in the conception, study design, execution, acquisition of data, analysis and interpretation, or in all these areas; took part in drafting, revising or critically reviewing the article; gave final approval of the version to be published; have agreed on the journal to which the article has been submitted; and agree to be accountable for all aspects of the work.

Consent for Publication

The authors confirm that the details of any images, videos, recordings, etc can be published, and that the authors providing consent have been shown the article contents to be published.

Funding

This research was supported by the National Natural Sciences Foundation of China (grant numbers 82074406).

Disclosure

The authors report no conflicts of interest in this work.

References

1. Global Initiative for Chronic Obstructive Lung Disease. Global strategy for the diagnosis, management, and prevention of chronic obstructive pulmonary disease, 2022 Available from: <http://www.goldcopd.org>. Accessed June 30, 2025.
2. Hou W, Hu S, Li C, et al. Cigarette smoke induced lung barrier dysfunction, EMT, and tissue remodeling: a possible link between COPD and lung cancer. *Biomed Res Int*. 2019;2019:2025636. doi:10.1155/2019/2025636
3. Sun T, Xia S, Junzhen W, et al. Inflammation and mechanism of pneumoblood barrier in hypoxic lung. *Chin J Lung Diseases*. 2013;6(06):547–550.
4. Hong JR, Zhang CY, Zhong WJ, et al. Epoxyeicosatrienoic acids alleviate alveolar epithelial cell senescence by inhibiting mitophagy through NOX4/Nrf2 pathway. *Biomed Pharmacother*. 2023;169:115937. doi:10.1016/j.biopha.2023.115937
5. Zhu L, Wu Z, Liu Y, et al. Acod1/itaconate activates Nrf2 in pulmonary microvascular endothelial cells to protect against the obesity-induced pulmonary microvascular endotheliopathy. *Respir Res*. 2024;25(1):205. doi:10.1186/s12931-024-02827-w
6. Barnes PJ. Oxidative stress-based therapeutics in COPD. *Redox Biol*. 2020;33:101544. doi:10.1016/j.redox.2020.101544
7. Pizzino G, Irrera N, Cucinotta M, et al. oxidative stress: harms and benefits for human health. *Oxid Med Cell Longev*. 2017;2017:8416763. doi:10.1155/2017/8416763
8. Li J, Baker J, Higham A, et al. COPD lung studies of Nrf2 expression and the effects of Nrf2 activators. *Inflammopharmacology*. 2022;30(4):1431–1443. doi:10.1007/s10787-022-00967-3
9. Zhu WT, Li CH, Dai TT, et al. Effect of allyl isothiocyanate on oxidative stress in COPD via the AhR / CYP1A1 and Nrf2 / NQO1 pathways and the underlying mechanism. *Phytomedicine*. 2023;114:154774. doi:10.1016/j.phymed.2023.154774
10. Fan X, Dong T, Yan K, et al. PM2.5 increases susceptibility to acute exacerbation of COPD via NOX4/Nrf2 redox imbalance-mediated mitophagy. *Redox Biol*. 2023;59:102587. doi:10.1016/j.redox.2022.102587
11. Li J, Xie Y, Zhao P, et al. A Chinese herbal formula ameliorates COPD by inhibiting the inflammatory response via downregulation of p65, JNK, and p38. *Phytomedicine*. 2021;83:153475. doi:10.1016/j.phymed.2021.153475
12. Tian Y, Li Y, Li J, et al. Bufei Yishen granule combined with acupoint sticking improves pulmonary function and morphometry in chronic obstructive pulmonary disease rats. *BMC Complement Altern Med*. 2015;15:266. doi:10.1186/s12906-015-0787-0
13. Tian Y, Li J, Li Y, et al. Effects of bufei yishen granules combined with acupoint sticking therapy on pulmonary surfactant proteins in chronic obstructive pulmonary disease rats. *Biomed Res Int*. 2016;2016:8786235. doi:10.1155/2016/8786235
14. Li J, Wang J, Li Y, et al. Effective-component compatibility of Bufei Yishen formula protects COPD rats against PM2.5-induced oxidative stress via miR-155/FOXO3a pathway. *Ecotoxicol Environ Saf*. 2021;228:112918. doi:10.1016/j.ecoenv.2021.112918
15. Li Y, Li SY, Li JS, et al. A rat model for stable chronic obstructive pulmonary disease induced by cigarette smoke inhalation and repetitive bacterial infection. *Biol Pharm Bull*. 2012;35(10):1752–1760. doi:10.1248/bpb.b12-00407
16. Rogliani P, Manzetti GM, Gholamalishahi S, et al. Impact of N-acetylcysteine on mucus hypersecretion in the airways: a systematic review. *Int J Chron Obstruct Pulmon Dis*. 2024;19:2347–2360. doi:10.2147/COPD.S474512
17. Xu K, Ma J, Lu R, et al. Effective-compound combination of Bufei Yishen formula III combined with ER suppress airway mucus hypersecretion in COPD rats: via EGFR/MAPK signaling. *Biosci Rep*. 2023;43(11):BSR20222669. doi:10.1042/BSR20222669
18. Li MY, Qin YQ, Tian YG, et al. Effective-component compatibility of Bufei Yishen formula III ameliorated COPD by improving airway epithelial cell senescence by promoting mitophagy via the NRF2/PINK1 pathway. *BMC Pulm Med*. 2022;22(1):434. doi:10.1186/s12890-022-02191-9
19. Tudor RM. Bringing light to chronic obstructive pulmonary disease pathogenesis and resilience. *Ann Am Thorac Soc*. 2018;15(Suppl 4):S227–S233. doi:10.1513/AnnalsATS.201808-583MG
20. Chang J, Chen Z, Zhao R, et al. Ion transport mechanisms for smoke inhalation-injured airway epithelial barrier. *Cell Biol Toxicol*. 2020;36(6):571–589. doi:10.1007/s10565-020-09545-1
21. Gane J, Stockley R. Mechanisms of neutrophil transmigration across the vascular endothelium in COPD. *Thorax*. 2012;67(6):553–561. doi:10.1136/thoraxjnl-2011-200088
22. Rincon M, Irvin CG. Role of IL-6 in asthma and other inflammatory pulmonary diseases. *Int J Biol Sci*. 2012;8(9):1281–1290. doi:10.7150/ijbs.4874
23. Takamiya R, Uchida K, Shibata T, et al. Disruption of the structural and functional features of surfactant protein A by acrolein in cigarette smoke. *Sci Rep*. 2017;7(1):8304. doi:10.1038/s41598-017-08588-5
24. Agudelo CW, Kumley BK, Area-Gomez E, et al. Decreased surfactant lipids correlate with lung function in chronic obstructive pulmonary disease (COPD). *PLoS One*. 2020;15(2):e0228279. doi:10.1371/journal.pone.0228279
25. Blanco I, Piccari L, Barberà JA. Pulmonary vasculature in COPD: the silent component. *Respirology*. 2016;21(6):984–994. doi:10.1111/resp.12772
26. A'na H, Jianhua F, Xindong X. Study of the variation in expression and the significance of markers for alveolar epithelial cells in bronchopulmonary dysplasia newborn rats. *Chin Pediatric Emerg Med*. 2017;24(2):132–136.

27. Sheng Y, Ping Z, Lei Y, et al. Expression of AQP1 and AQP5 is decreased in the alveolar-capillary membrane in rats with acute lung injury. *Chin J Comparative Med.* 2016;26(8):70–74,90.
28. Yoshida M, Whitsett JA. Alveolar macrophages and emphysema in surfactant protein-D-deficient mice. *Respirology.* 2006;11:S37–40. doi:10.1111/j.1440-1843.2006.00806.x
29. Lv MY, Qiang LX, Wang BC, et al. Complex evaluation of surfactant protein A and D as biomarkers for the severity of COPD. *Int J Chron Obstruct Pulmon Dis.* 2022;17:1537–1552. doi:10.2147/COPD.S366988
30. Kutikhin AG, Shishkova DK, Velikanova EA, et al. Endothelial dysfunction in the context of blood-brain barrier modeling. *J Evol Biochem Physiol.* 2022;58(3):781–806. doi:10.1134/S0022093022030139
31. Kutikhin AG, Tupikin AE, Matveeva VG, et al. human peripheral blood-derived endothelial colony-forming cells are highly similar to mature vascular endothelial cells yet demonstrate a transitional transcriptomic signature. *Cells.* 2020;9(4):876. doi:10.3390/cells9040876
32. Zeng M, Li Y, Jiang Y, et al. Local and systemic oxidative stress status in chronic obstructive pulmonary disease patients. *Can Respir J.* 2013;20(1):35–41. doi:10.1155/2013/985382
33. Zinellu E, Zinellu A, Fois AG, et al. Circulating biomarkers of oxidative stress in chronic obstructive pulmonary disease: a systematic review. *Respir Res.* 2016;17(1):150. doi:10.1186/s12931-016-0471-z
34. Klaassen CD, Reisman SA. Nrf2 the rescue: effects of the antioxidative/electrophilic response on the liver. *Toxicol Appl Pharmacol.* 2010;244(1):57–65. doi:10.1016/j.taap.2010.01.013
35. Cen J, Zhao N, Huang WW, et al. Polyamine analogue QMA attenuated ischemic injury in MCAO rats via ERK and Akt activated Nrf2/HO-1 signaling pathway. *Eur J Pharmacol.* 2019;844:165–174. doi:10.1016/j.ejphar.2018.12.015
36. Osama A, Zhang J, Yao J, et al. Nrf2: a dark horse in Alzheimer's disease treatment. *Ageing Res Rev.* 2020;64:101206. doi:10.1016/j.arr.2020.101206
37. Loboda A, Damulewicz M, Pyza E, et al. Role of Nrf2/HO-1 system in development, oxidative stress response and diseases: an evolutionarily conserved mechanism. *Cell Mol Life Sci.* 2016;73(17):3221–3247. doi:10.1007/s00018-016-2223-0
38. Akino N, Wada-Hiraike O, Terao H, et al. Activation of Nrf2 might reduce oxidative stress in human granulosa cells. *Mol Cell Endocrinol.* 2018;470:96–104. doi:10.1016/j.mce.2017.10.002
39. Du Y, Zhang H, Xu Y, et al. Association among genetic polymorphisms of GSTP1, HO-1, and SOD-3 and chronic obstructive pulmonary disease susceptibility. *Int J Chron Obstruct Pulmon Dis.* 2019;14:2081–2088. doi:10.2147/COPD.S213364
40. Zhu J, Bi Z, Yang T, et al. Regulation of PKM2 and Nrf2-ARE pathway during benzoquinone induced oxidative stress in yolk sac hematopoietic stem cells. *PLoS One.* 2014;9(12):e113733. doi:10.1371/journal.pone.0113733

International Journal of Chronic Obstructive Pulmonary Disease

Publish your work in this journal

The International Journal of COPD is an international, peer-reviewed journal of therapeutics and pharmacology focusing on concise rapid reporting of clinical studies and reviews in COPD. Special focus is given to the pathophysiological processes underlying the disease, intervention programs, patient focused education, and self management protocols. This journal is indexed on PubMed Central, MedLine and CAS. The manuscript management system is completely online and includes a very quick and fair peer-review system, which is all easy to use. Visit <http://www.dovepress.com/testimonials.php> to read real quotes from published authors.

Submit your manuscript here: <https://www.dovepress.com/international-journal-of-chronic-obstructive-pulmonary-disease-journal>

Dovepress
Taylor & Francis Group